Published in final edited form as:
Neurobiol Dis. 2014 February ; 62: . doi:10.1016/j.nbd.2013.10.001.

Pacemaker GABA Synaptic Activity May Contribute to Network Synchronization in Pediatric Cortical Dysplasia

Carlos Cepeda[1], **Jane Y. Chen**[1], **Joyce Y. Wu**[2], **Robin S. Fisher**[1], **Harry V. Vinters**[3], **Gary W. Mathern**[1,4], and **Michael S. Levine**[1]

[1]Intellectual and Developmental Disabilities Research Center, Brain Research Institute, University of California Los Angeles

[2]Division of Pediatric Neurology, Mattel Children's Hospital, David Geffen School of Medicine, University of California Los Angeles

[3]Department of Neurology, Section of Neuropathology, Mattel Children's Hospital, David Geffen School of Medicine, University of California Los Angeles

[4]Department of Neurology, Section of Neurosurgery and Psychiatry & BioBehavioral Medicine, Mattel Children's Hospital, David Geffen School of Medicine, University of California Los Angeles

Abstract

Spontaneous pacemaker γ-aminobutyric acid (GABA) receptor-mediated synaptic activity (PGA) occurs in a subset of tissue samples from pediatric epilepsy surgery patients. In the present study, based on single-cell electrophysiological recordings from 120 cases, we describe the etiologies, cell types, and primary electrophysiological features of PGA. Cells displaying PGA occurred more frequently in the areas of greatest anatomical abnormality in cases of focal cortical dysplasia (CD), often associated with hemimegalencephaly (HME), and only rarely in non-CD etiologies. PGA was characterized by rhythmic synaptic events (5–10 Hz) and was observed in normal-like, dysmorphic cytomegalic, and immature pyramidal neurons. PGA was action potential-dependent, mediated by $GABA_A$ receptors, and unaffected by antagonism of glutamate receptors. We propose that PGA is a unique electrophysiological characteristic associated with CD and HME. It could represent an abnormal signal that may contribute to epileptogenesis in malformed postnatal cortex by facilitating pyramidal neuron synchrony.

Keywords

Pediatric Epilepsy; Cortical Dysplasia; Synaptic Activity; GABA; Synchrony; Development

Introduction

Cortical Dysplasia (CD) is a neurodevelopmental disorder characterized by cortical dyslamination and, in severe cases, the presence of aberrant cells including dysmorphic neurons and balloon cells (Taylor et al., 1971). CD is the most common pathological

Address for Correspondence: Carlos Cepeda, Ph.D., Intellectual and Developmental Disabilities Research Center, Semel Institute for Neuroscience, Room 58-258, UCLA School of Medicine, 760 Westwood Plaza, Los Angeles, CA 90024, Tel: (310) 206-0861, Fax: (310) 206-5060, ccepeda@mednet.ucla.edu.

substrate in pediatric epilepsy surgery patients (Harvey et al., 2008; Lerner et al., 2009; Mathern et al., 1999) and seizures are usually refractory to antiepileptic drugs (AEDs) (Barkovich et al., 2012). Tuberous sclerosis complex (TSC), a genetic autosomal dominant disorder characterized by cortical and subcortical tubers, displays similar histopathologic features as severe CD, and also presents with a high incidence of epilepsy.

Previous studies have characterized some of the morphological, electrophysiological, and molecular biological features of abnormal cells in CD and TSC (Cepeda et al., 2003; Crino, 2010). For example, our group demonstrated that balloon cells are unable to generate epileptic discharges due to the lack of ionic conductances required for the generation of action potentials and do not receive synaptic inputs (Cepeda et al., 2005b). In contrast, dysmorphic cytomegalic pyramidal neurons display increased Ca^{2+} conductances and reduced Mg^{2+} sensitivity, suggesting they have a role in epileptogenesis (Andre et al., 2004; Andre et al., 2007; Cepeda et al., 2005a; Cepeda et al., 2006; Cepeda et al., 2005b; Cepeda et al., 2007; Cepeda et al., 2003; Mathern et al., 2000). We also demonstrated that the frequency of spontaneous $GABA_A$ receptor-mediated synaptic activity, relative to glutamate receptor-mediated synaptic activity, is increased in CD compared with non-CD cases (Cepeda et al., 2005a). This led us to propose a developmental dysmaturity hypothesis of epileptogenesis in CD (Cepeda et al., 2006).

Other findings from our investigations have shown that CD tissue contains elements of abnormal neuronal maturation. For example, CD cases often contain clusters of immature pyramidal neurons showing signs of increased membrane excitability (Cepeda et al., 2007). In a subpopulation of immature pyramidal neurons we observed the occurrence of spontaneous, rhythmic GABAergic synaptic events (Cepeda et al., 2003). As rhythmic activity could promote epileptogenesis by contributing to network synchronization, the present study was designed to further investigate the incidence and principal characteristics of pacemaker GABA synaptic activity (PGA) in pediatric epilepsy surgery cases.

Methods

The research protocols were approved by the Institutional Review Board of the Human Protection Research Committee at the University of California Los Angeles (UCLA). Informed consent to use the surgically resected tissue for research was obtained from the parents or legal guardians. This study is not a clinical trial and it is not recorded in any public registry.

Cohort

The present study includes 120 cases of pharmaco-resistant pediatric epilepsy patients that underwent surgical resection of the abnormal, epileptogenic areas. This cohort represents a subset of all our surgical cases (n=267) with slice electrophysiological recordings spanning over 20 years. Cases for this study were chosen based on the criterion that spontaneous GABA receptor-mediated synaptic activity was recorded in at least 2 pyramidal neurons (usually 4–5) from each case.

Based on histopathology, cases were classified into CD and non-CD groups as previously described (Cepeda et al., 2005a; Cepeda et al., 2003). The CD group was subsequently divided according to the recent International League Against Epilepsy (ILAE) consensus classification: CD Type I, where only cytoarchitectural abnormalities are observed, either as radial (Type Ia) or tangential (Type Ib) dyslamination; CD Type II where, in addition to dyslamination, abnormal dysmorphic neurons (Type IIa) and balloon cells are observed (Type IIb) and CD Type III, where dysplasia occurs in association with other epileptogenic

pathologies such as hippocampal sclerosis (Type IIIa) or tumors (Type IIIb) (Blumcke et al., 2011).

Non-CD pathologies included Rasmussen encephalitis (RE), ulegyria, cystic encephalopathy, Sturge-Weber, and stroke. In 6 cases no epileptogenic histopathology was found or only minimal Chaslin's gliosis. At the time of surgery, patients were undergoing pharmacologic treatment with AEDs that included, in descending order, topiramate, phenobarbital, lamotrigine, zonisamide, clonazepam, carbamazepine and adrenocorticotropic hormone (ACTH).

Pre-surgical evaluation and clinical information

The standardized evaluation included clinical history, neurological examinations, and scalp EEG video-recordings (Hauptman et al., 2012; Hemb et al., 2010; Mathern et al., 1999). Neuroimaging studies included magnetic resonance imaging (MRI) and 18-Fluoro-deoxyglucose positron emission tomography (FDG-PET) (Salamon et al., 2008). Clinical data were obtained from the medical records and included: age at seizure onset, age at surgery, type of operation (hemispherectomy, multilobar, lobar/focal), side of operation, gender, seizure frequency, and number of AEDs (Hemb et al., 2010). Also recorded was the region of the brain sampled for *in vitro* cellular electrophysiology studies.

Electrophysiological and morphological methods

Detailed electrophysiological and morphological methods have been described previously (Cepeda et al., 2012; Cepeda et al., 2003). In brief, neocortical tissue samples were excised for *in vitro* electrophysiology and were classified as most (MA) and least abnormal (LA) based on neuroimaging (MRI, PET) and electrocorticography (ECoG). Samples were removed microsurgically and directly placed in ice-cold, low Ca^{2+} artificial cerebrospinal fluid (ACSF) containing (in mM); NaCl 130, $NaHCO_3$ 26, KCl 3, $MgCl_2$ 5, NaH_2PO_4 1.25, $CaCl_2$ 1.0, glucose 10 (pH 7.2–7.4). Within 5–10 min, slices were cut and incubated in regular ACSF (in this solution $CaCl_2$ was increased to 2 mM and $MgCl_2$ was decreased to 2 mM) for at least 1h. Patch electrodes were filled with (in mM) Cs-methanesulfonate 125, NaCl 4, KCl 3, $MgCl_2$ 1, MgATP 5, ethylene glycol-bis (β-aminoethyl ether)-N,N,N′,N′-tetraacetic acid (EGTA) 9, HEPES 8, GTP 1, phosphocreatine 10 and leupeptine 0.1 (pH 7.25–7.3, osmolality 280–290 mOsm) for voltage clamp recordings. Electrodes also contained 0.2% biocytin in the internal solution to label recorded cells. Cells were initially held at −70 mV in voltage clamp mode. After characterizing the basic membrane properties of the cell (capacitance, input resistance and decay time constant using a 10 mV depolarizing step voltage command) spontaneous excitatory (EPSCs) and inhibitory (IPSCs) postsynaptic currents were recorded for 3 min. Spontaneous EPSCs were partially isolated by holding the membrane at −70 mV and IPSCs were isolated by holding the membrane at +10 mV in the presence of appropriate receptor antagonists [amino-5-phosphonovaleric acid (APV) for N-methyl-D-aspartate (NMDA) and 6-cyano-7-nitroquinoxaline-2,3-dione (CNQX) or 2,3-dihydroxy-6-nitro-7-sulfamoyl-benzo[f]quinoxaline-2,3-dione (NBQX) for non-NMDA glutamate receptors] and miniature (m)IPSCs were isolated by addition of tetrodotoxin (TTX, 1 μM) to the external solution. Frequency of spontaneous PSCs, kinetic and correlation analyses were performed using the Mini Analysis program (Cepeda et al., 2005a).

Correlation analysis

Only rhythmic events that define PGA were included in the correlation analyses. For each cell, the minimum threshold was set above the level of random spontaneous GABA synaptic events. Autocorrelations were assigned different ratings based on correlation coefficients and visual inspection of the histograms from each cell. A histogram with high

autocorrelation (A and B) had correlation coefficients >0.2 (first peak range 0.207–0.667) and showed high-amplitude oscillating peaks at each lag period, while a low autocorrelation (C and D) had correlation coefficients <0.2 (first peak range 0.051–0.149) and showed only 1–2 low-amplitude peaks. Cells with no correlation showed no peaks except at the origin (lag 0) where the correlation is always 1 (Fig. 3).

Cell types

Normal and abnormal neuronal types in CD etiologies were separated following well-established criteria (Blumcke et al., 2011; Cepeda et al., 2003; Taylor et al., 1971). Based on biocytin staining and electrophysiological features cells were classified as normal-like, dysmorphic cytomegalic, or immature pyramidal neurons (Cepeda et al., 2003). Normal-like pyramidal neurons had medium-sized somata, typical apical and basilar dendrites and, in most cases, abundant spines. They represented the most prevalent type in CD and non-CD cases. Dysmorphic pyramidal neurons, an essential component of CD Types IIa and IIb, displayed abnormally large somata and nuclei, hence also called cytomegalic. Immature neurons had a smaller somatic diameter and reduced number of dendrites and spines compared with normal-like pyramidal neurons. Based on electrophysiological membrane properties, dysmorphic cytomegalic pyramidal neurons had larger cell membrane capacitance and lower input resistance, whereas immature pyramidal neurons had smaller capacitance and higher input resistance compared with normal-like pyramidal neurons (Table II).

NeuN immunocytochemistry

Freshly cut paraffin sections (~6 μm thickness) were heated overnight (60° C), deparaffinized through xylenes and graded concentrations of ethanol, washed in deionized water, then pretreated by microwaving in citrate buffer. Endogenous peroxidase was blocked by immersing slides in 3% hydrogen peroxide. Primary antibody (NeuN, Millipore MAB377) was used at a dilution of 1:200, and slides incubated at room temperature for 80 min. After washing the treated slides, secondary (anti-mouse) antibody was applied for 15 min prior to washing in buffer. Diaminobenzidine chromogen was added for several minutes, followed by a distilled water wash, counterstaining with hematoxylin and coverslipping.

Statistics

Values are presented as mean±standard error of the mean (SEM). Differences were considered statistically significant if $p<0.05$. Statistical differences between groups were examined using Chi-square or appropriate one- or two-way ANOVAs followed by Bonferroni *post hoc* tests.

Results

PGA occurs in the most abnormal regions of CD and HME cases

In the cohort that met our inclusion criteria (n=120 cases, average age 3.8±0.3 yr, range 0.2–14.2 yr), cells displaying PGA were mostly found in patients with CD. An example of ECoG, MRI, and histopathology from a CD Type IIb case (3.6 yr) that displayed PGA at the cellular level is illustrated in Fig. 1(A–C). In patients with CD, 27 of 80 (34%) cases displayed PGA (Table I). In contrast, only 2 of 25 non-CD cases displayed PGA (8%; $p=0.01$, Chi-square). As might be expected from previous reports (Cepeda et al., 2005a), age at surgery was younger for CD (2.9±0.4 yr) compared with non-CD (6.2±0.7 yr; $p<0.001$) patients. To exclude age as a contributing factor, we performed a logistic regression analysis where age at surgery and CD versus non-CD were independent variables and cells showing

PGA versus no-PGA was the dependent variable. This analysis found that cells displaying PGA were associated with CD (p=0.024) but not with age (p=0.244). In patients with TSC, PGA was observed in 2 of 15 cases (13%) and the mean age (4.1±0.8 yr) was not significantly different compared with CD and non-CD cases.

The occurrence of PGA showed slight differences by CD subtype. PGA was observed in 7 of 26 (27%) cases presenting with CD Type I, in 17 of 50 cases (34%) with CD Type IIa/b, and in 3 of 4 cases (75%) with CD Type IIIb (CD associated with ganglioglioma or dysembryoplastic neuroepithelial tumor) (Table I). However, the differences in proportion of PGA among CD subtypes (p=0.17) or between CD Type I and CD Type II (p=0.53, Chi-square) were not statistically significant. Interestingly, 8 of 27 CD cases (30%) displaying PGA also had hemimegalencephaly (HME, Suppl. Table I). For non-CD cases, PGA was observed in 1 of 8 (12.5%) RE patients and 1 of 6 (16.7%) cases without significant pathology (Suppl. Table I).

Cells showing PGA were more prevalent in the MA compared with the LA brain samples (Suppl. Table I). Of 33 cells (from 31 cases) displaying PGA, 26 (79%) were found in the MA compared with 7 in the LA samples (p<0.001, Chi-square). Cells displaying PGA were equally distributed among cerebral regions except for the occipital lobe, which was only rarely sampled in our pediatric surgery cases. Thus, 12 cells were recorded in the frontal lobe, 12 in the temporal lobe, 8 in the parietal lobe, and 1 in the occipital lobe.

Electrophysiological features of PGA

PGA was produced by activation of $GABA_A$ receptors as it was completely abolished by bicuculline (BIC) (Fig. 2A and 6D). Furthermore, its reversal potential was near the predicted equilibrium potential for Cl^- (~−60 mV in our recording conditions). PGA was visible at a wide range of holding potentials, even at −70 mV (our standard holding potential), despite being close to the Cl^- equilibrium potential. Upon depolarization, the amplitude of rhythmic events increased linearly as the driving force for Cl^- also increased (Fig. 2C). However, in some cells the current-voltage relationship displayed some degree of rectification (Fig. 2D). At a holding potential of +10 mV (our preferred potential to maximize spontaneous GABAergic synaptic currents), the amplitude of PGA was in general 5–6 times greater than that of spontaneous random events (Fig. 3A, **arrows).** The average amplitude of PGA at this holding potential was 210.5±43.5 pA (range of 32–721 pA) while that of random events was 34.6±3.9 pA (range of 7–71 pA, n=17 neurons). This possibly implies that PGA may represent the synchronous firing of multiple interneurons. Alternatively, it is possible that pacemaker GABA inputs arrive preferentially at or closer to the soma and/or proximal dendrites. Addition of glutamate receptor antagonists (CNQX or NBQX and APV, n=3) to the perfusate did not affect the frequency or amplitude of PGA (Fig. 5B). However, PGA depends on action potential firing as it was completely abolished by Na^+ channel block with TTX (n=3). After TTX application only random, low-amplitude mIPSCs remained (Fig. 5B, C).

A key characteristic of PGA was its clock-like nature (i.e., displayed little variations in frequency, see Suppl. Video clip). It manifested either as a continuous rhythm throughout the duration of the recording or, less frequently, as short (~10–30 sec) episodes of rhythmic activity. Although the frequency of PGA varied among cells, the usual range was between 5–10 Hz, with an average of 7.5±0.6 Hz. The predominant time interval was between 100–200 ms, which corresponded to the frequency range of 5–10 Hz.

To demonstrate the non-random nature of PGA we used an autocorrelation analysis. This analysis demonstrated varying degrees of autocorrelation in spontaneous synaptic GABAergic events (Fig. 3B). Based on the correlation coefficient and visual inspection of

the histograms, we classified neurons displaying PGA into 4 categories; very high (A; n=9), high (B; n=10), medium (C; n=7), and low (D; n=7) degree of autocorrelation (Fig. 3 and Suppl. Table I). As expected, the difference in correlation coefficients among groups was statistically significant ($p<0.001$), whereas there was no difference between degree of autocorrelation and pathology ($p=0.485$, two-way RM ANOVA) or age ($p=0.485$, Pearson Product Moment Correlation). Cells with the highest degree of autocorrelation (A) were found in CD Type I (n=4), CD Type IIa/b (n=4), and CD Type IIIb (n=1).

In two additional cases (one with CD Type I and the other with polymicrogyria and HME) not included in the present cohort as PGA did not occur spontaneously, we observed that it could be induced by 4-aminopyridine (4-AP, 100 μM), a K^+ channel blocker that increases neurotransmitter release and generates rhythmic oscillations. This probably indicates that 4-AP can affect interneuron firing and facilitate the occurrence of network synchronization and PGA.

Cell types displaying PGA

In the 31 cases displaying PGA, a total of 210 cells were recorded electrophysiologically. Based on morphological (using IR-DIC during slice recordings, and biocytin as an intracellular marker) and electrophysiological membrane properties, 158 cells were classified as normal-like, 15 as dysmorphic cytomegalic, and 14 as immature pyramidal neurons. The remainder (n=23) were non-pyramidal neurons. The vast majority of cells displaying PGA were pyramidal (33 of 187, 18%). They were normal-like (24 of 158, 15%), immature (4 of 14, 29%) and dysmorphic cytomegalic (5 of 15, 33%). There were no statistically significant differences in basic membrane properties, including cell capacitance, input resistance and decay time constant, between PGA and non-PGA pyramidal neurons (Table II).

Successful biocytin labeling was obtained from 20 pyramidal neurons (18 cases) displaying PGA; 14 normal-like, 4 dysmorphic cytomegalic and 2 immature. While normal-like pyramidal neurons with PGA had normal-sized somata, most displayed morphological changes. These consisted of widespread swellings (blebbing) and constrictions restricted to the apical dendrite and dendritic shafts (Fig. 7). Mild to severe blebbing was observed in 9 of 20 PGA cells (45%). By comparison, in normal-like pyramidal neurons (n=75) not showing PGA but recorded from the same cases where at least once cell displayed PGA (n=24), blebbing occurred in 10 of 75 cells (13.3%). In normal-like pyramidal neurons (n=56) from non-CD cases without PGA (n=19), blebbing was observed in only two cells (3.5%). The difference among groups was highly significant ($p<0.001$, Chi-square). Another common characteristic of normal-like pyramidal neurons with PGA was a scarcity of dendritic spines. These anatomical findings suggest that PGA pyramidal neurons display greater morphological abnormalities compared with non-PGA cells.

In the same patients where PGA occurred, 23 non-pyramidal, putative interneurons also were recorded. Of these cells, only one (4.3%) displayed PGA (~10 Hz). This interneuron was from a CD Type IIa case with HME. Most interneurons corresponded to the basket type and most were fast-spiking. Only three interneurons fired spontaneous, regular action potentials in the range of 5–10 Hz, i.e., similar to the frequency of PGA (data not shown).

Discussion

The present study provides a characterization of neurons that display PGA from pediatric epilepsy surgery patients. Cells displaying PGA occurred more frequently found in cases of CD compared with non-CD etiologies, and were more related to histopathology rather than the younger age at surgery. For CD cases, within subject comparisons demonstrated that the

majority of cells displaying PGA occurred in the MA cortical samples. PGA was characterized by rhythmic, clock-like events (5–10 Hz), was action potential dependent, mediated by $GABA_A$ receptors, and unaffected by blockade of glutamate receptors. It was observed in different cells types including normal-like, dysmorphic cytomegalic, and immature pyramidal neurons. Only one fast-spiking interneuron displayed this activity. Normal-like pyramidal neurons displaying PGA showed abnormal dendritic morphology including membrane blebbing and sparsity of spines (Isokawa and Levesque, 1991).

The most remarkable feature of PGA is its clock-like rhythmicity and high degree of autocorrelation. Neurotransmitter release is, for the most part, a stochastic process that follows a Poisson distribution, although divergence from this norm, particularly at central nervous synapses, may occur (Abenavoli et al., 2000). Here we demonstrate that PGA is determined by presynaptic interneuron firing because after blockade of Na^+ channels the remaining mIPSCs display the more typical non-correlated, Poisson-like distribution. Several factors may contribute to make PGA such a prominent signal that rises above small-amplitude, random synaptic events. In the case of immature pyramidal neurons, high input resistance could enhance the likelihood of inducing PGA. The topography of presynaptic terminals also could play a role; inputs closer to the soma would be more likely to induce PGA. Tight synaptic coupling could be enhanced by scarcity of glutamatergic connections as may occur in early development (i.e., before the presence of distal dendrites and spines), or in CD.

Which could be the most likely generator of PGA? There are about 20 different classes of GABAergic interneurons in the cerebral cortex (Monyer and Markram, 2004). The most common are, based on dendritic or axonal morphology, basket cells, chandelier, Martinotti, and double-bouquet or bitufted interneurons. Based on firing patterns, interneurons can be fast-spiking, regular spiking, irregular spiking and bursting. The possible interneurons generating PGA have to fulfill several criteria: a) They should fire spontaneously at a frequency of ~5–10 Hz, b) They should innervate the soma and proximal basal and/or apical dendrites of target neurons, c) They should display little or no adaptation, and d) They should not produce bursting activity. Based on these criteria, as well as the current classification of cortical interneurons (Petilla Interneuron Nomenclature et al., 2008), we would expect that the generator of PGA is not a fast-spiking, bursting, or an adapting interneuron. In addition, Martinotti cells seem to innervate layer I neurons preferentially and chandelier cells innervate the proximal axon of pyramidal neurons. These criteria leave primarily the regular spiking interneurons as the likely source of PGA. These cells include the bitufted or double-bouquet interneurons. This type of interneuron is numerous in primates and rare or non-existent in rodents. They represent a source of abundant GABAergic synapses on dendritic shafts and spines on oblique dendrites of pyramidal neurons and are considered a key element in the microcolumnar organization typical of primates (DeFelipe, 2011).

PGA is a highly synchronized signal that affects cellular excitability. In current clamp recordings, at least in immature pyramidal neurons, we previously demonstrated that rhythmic, depolarizing GABA synaptic events can facilitate the occurrence of action potentials and addition of a $GABA_A$ receptor antagonist abolishes firing arising from these events (Cepeda et al., 2007). Sub-threshold GABA depolarizations may induce a rise in cytosolic Ca^{2+} (Ben-Ari et al., 2007; Obrietan and van den Pol, 1997), which in turn favors neuronal firing. If PGA is depolarizing in immature, normal-like, and dysmorphic cytomegalic pyramidal neurons, even in a subset of these neurons, it could increase the likelihood of cell firing. PGA may thus be able to synchronize and entrain other cells within the local network. As the occurrence of PGA is action potential-dependent, the GABA interneurons that generate this activity have the capability of firing in a rhythmic fashion and

could be essential to synchronize large groups of pyramidal neurons, similar to a synchronous firing chain (Abeles, 1982). This process could contribute to seizure generation in CD cases.

There are a number of clinical and experimental limitations that could affect the interpretation of our results. First, all of the surgery cases were receiving AEDs and many of these drugs modulate $GABA_A$ receptor function. However, the finding that PGA occurred mostly in CD compared with non-CD cases that were using similar medication argues against a substantial impact of AEDs on the presence of PGA. Furthermore, the vast majority of interneurons possess pacemaker capabilities that depend primarily on intrinsic voltage-gated conductances (Wu et al., 2005). If at all, AEDs are more likely to affect GABA reuptake, IPSC amplitude and/or kinetics. It also is improbable that ACTH affected interneuron firing as its main action is the stimulation of steroid hormone secretion and cholesterol delivery to mitochondria.

Another caveat that may affect our morphological findings is the fact that neurons undergo alterations depending on the slicing and incubation procedures (Kirov et al., 2004). However, the fact that the vast majority of normal-like pyramidal neurons from non-CD cases, in particular those with minimal pathology and Chaslin's gliosis, showed normal morphology, makes this possibility unlikely. Also, the idea that PGA is depolarizing in immature and dysmorphic cytomegalic neurons needs to await further support from perforated patch recordings that do not alter the Cl^- reversal potential. Nonetheless, measurement of GABA reversal potentials in slices is fraught with significant problems due to the slicing procedure, which also could alter neuronal physiology, particularly near the surface. A recent study demonstrated that in more intact preparations GABA is hyperpolarizing even in immature neurons and that depolarizing GABA effects are more likely the result of trauma caused by the slicing procedure (Dzhala et al., 2012). Thus far, successful perforated patch recordings in human tissue slices are scarce (Talos et al., 2012). Interestingly, in this study from a TSC case (1.4 yr old) GABA synaptic events were depolarizing, supporting the idea that in dysplastic tissue GABA could be excitatory. It is tempting to speculate that morphological abnormalities occurring in normal-like pyramidal neurons from CD patients could facilitate depolarizing actions of GABA. Additional studies will be required to assess the role of PGA in more intact preparations.

Supplementary Material

Refer to Web version on PubMed Central for supplementary material.

Acknowledgments

The authors would like to thank the patients and their parents for allowing use of resected specimen for experimentation. We also thank the UCLA Hospital Pediatric Neurology staff for their assistance. Drs. Jorge Flores-Hernández, Gloria J. Klapstein, Raymond S. Hurst, Max Kleiman-Weiner, Irene Yamazaki, Besim Uzgil and Galatia J. Cepeda participated in data collection and analysis. My N. Huynh did the biocytin processing and Donna Crandall helped with the illustrations. This work was supported by NIH grants NS 38992 (GWM, CC, MSL) and NS 51637 (JYW). HVV was supported in part by the University of California Pediatric Neuropathology Consortium.

References

Abeles, M. Local Cortical Circuits: An Electrophysiological Study. Springer-Verlag; Berlin Heidelberg New York: 1982.

Abenavoli A, et al. Mechanisms of spontaneous miniature activity at CA3-CA1 synapses: evidence for a divergence from a random Poisson process. Biol Bull. 2000; 199:184–6. [PubMed: 11081726]

Andre VM, et al. NMDA receptor alterations in neurons from pediatric cortical dysplasia tissue. Cereb Cortex. 2004; 14:634–46. [PubMed: 15054078]

Andre VM, et al. Cytomegalic interneurons: a new abnormal cell type in severe pediatric cortical dysplasia. J Neuropathol Exp Neurol. 2007; 66:491–504. [PubMed: 17549009]

Barkovich AJ, et al. A developmental and genetic classification for malformations of cortical development: update. 2012. Brain. 2012; 135:1348–69. [PubMed: 22427329]

Ben-Ari Y, et al. GABA: a pioneer transmitter that excites immature neurons and generates primitive oscillations. Physiol Rev. 2007; 87:1215–84. [PubMed: 17928584]

Blumcke I, et al. The clinicopathologic spectrum of focal cortical dysplasias: a consensus classification proposed by an ad hoc Task Force of the ILAE Diagnostic Methods Commission. Epilepsia. 2011; 52:158–74. [PubMed: 21219302]

Cepeda C, et al. Pediatric cortical dysplasia: correlations between neuroimaging, electrophysiology and location of cytomegalic neurons and balloon cells and glutamate/GABA synaptic circuits. Dev Neurosci. 2005a; 27:59–76. [PubMed: 15886485]

Cepeda C, et al. Enhanced GABAergic network and receptor function in pediatric cortical dysplasia Type IIB compared with Tuberous Sclerosis Complex. Neurobiol Dis. 2012; 45:310–21. [PubMed: 21889982]

Cepeda C, et al. Epileptogenesis in pediatric cortical dysplasia: the dysmature cerebral developmental hypothesis. Epilepsy Behav. 2006; 9:219–35. [PubMed: 16875879]

Cepeda C, et al. Are cytomegalic neurons and balloon cells generators of epileptic activity in pediatric cortical dysplasia? Epilepsia. 2005b; 46(Suppl 5):82–8. [PubMed: 15987258]

Cepeda C, et al. Immature neurons and GABA networks may contribute to epileptogenesis in pediatric cortical dysplasia. Epilepsia. 2007; 48(Suppl 5):79–85. [PubMed: 17910585]

Cepeda C, et al. Morphological and electrophysiological characterization of abnormal cell types in pediatric cortical dysplasia. J Neurosci Res. 2003; 72:472–86. [PubMed: 12704809]

Chassoux F, et al. Stereoelectroencephalography in focal cortical dysplasia: a 3D approach to delineating the dysplastic cortex. Brain. 2000; 123(Pt 8):1733–51. [PubMed: 10908202]

Crino PB. The pathophysiology of tuberous sclerosis complex. Epilepsia. 2010; 51(Suppl 1):27–9. [PubMed: 20331708]

DeFelipe J. The evolution of the brain, the human nature of cortical circuits, and intellectual creativity. Front Neuroanat. 2011; 5:29. [PubMed: 21647212]

Dzhala V, et al. Traumatic alterations in GABA signaling disrupt hippocampal network activity in the developing brain. J Neurosci. 2012; 32:4017–31. [PubMed: 22442068]

Gambardella A, et al. Usefulness of focal rhythmic discharges on scalp EEG of patients with focal cortical dysplasia and intractable epilepsy. Electroencephalogr Clin Neurophysiol. 1996; 98:243–9. [PubMed: 8641147]

Harvey AS, et al. Defining the spectrum of international practice in pediatric epilepsy surgery patients. Epilepsia. 2008; 49:146–55. [PubMed: 18042232]

Hauptman JS, et al. Pediatric epilepsy surgery: long-term 5-year seizure remission and medication use. Neurosurgery. 2012; 71:985–93. [PubMed: 22895408]

Hemb M, et al. Improved outcomes in pediatric epilepsy surgery: the UCLA experience, 1986–2008. Neurology. 2010; 74:1768–75. [PubMed: 20427752]

Isokawa M, Levesque MF. Increased NMDA responses and dendritic degeneration in human epileptic hippocampal neurons in slices. Neurosci Lett. 1991; 132:212–6. [PubMed: 1664504]

Kirov SA, et al. Dendritic spines disappear with chilling but proliferate excessively upon rewarming of mature hippocampus. Neuroscience. 2004; 127:69–80. [PubMed: 15219670]

Lerner JT, et al. Assessment and surgical outcomes for mild type I and severe type II cortical dysplasia: a critical review and the UCLA experience. Epilepsia. 2009; 50:1310–35. [PubMed: 19175385]

Mathern GW, et al. Neurons recorded from pediatric epilepsy surgery patients with cortical dysplasia. Epilepsia. 2000; 41(Suppl 6):S162–7. [PubMed: 10999538]

Mathern GW, et al. Postoperative seizure control and antiepileptic drug use in pediatric epilepsy surgery patients: the UCLA experience, 1986–1997. Epilepsia. 1999; 40:1740–9. [PubMed: 10612338]

Monyer H, Markram H. Interneuron Diversity series: Molecular and genetic tools to study GABAergic interneuron diversity and function. Trends Neurosci. 2004; 27:90–7. [PubMed: 15102488]

Obrietan K, van den Pol AN. GABA activity mediating cytosolic Ca2+ rises in developing neurons is modulated by cAMP-dependent signal transduction. J Neurosci. 1997; 17:4785–99. [PubMed: 9169537]

Petilla Interneuron Nomenclature G et al. Petilla terminology: nomenclature of features of GABAergic interneurons of the cerebral cortex. Nat Rev Neurosci. 2008; 9:557–68. [PubMed: 18568015]

Salamon N, et al. FDG-PET/MRI coregistration improves detection of cortical dysplasia in patients with epilepsy. Neurology. 2008; 71:1594–601. [PubMed: 19001249]

Talos DM, et al. Altered inhibition in tuberous sclerosis and type IIb cortical dysplasia. Ann Neurol. 2012; 71:539–51. [PubMed: 22447678]

Taylor DC, et al. Focal dysplasia of the cerebral cortex in epilepsy. J Neurol Neurosurg Psychiatry. 1971; 34:369–87. [PubMed: 5096551]

Wu J, et al. Electrophysiological properties of human hypothalamic hamartomas. Ann Neurol. 2005; 58:371–82. [PubMed: 16130091]

Clinical relevance

Postnatal CD tissue may offer a glimpse into synaptic mechanisms operational in the developing, albeit abnormal, brain. We propose that the presence of PGA in certain forms of pediatric epilepsy represents an abnormal signal that may play an important role in neuronal synchronization contributing to epileptogenesis in the malformed postnatal brain. In CD, one of the most striking observations at the EEG level is the occurrence of continuous rhythmic or pseudorhythmic spikes and polyspikes (Chassoux et al., 2000). Their average frequency is astonishingly close to the PGA recorded in the present study. Further, continuous and rhythmic epileptiform discharges have proven to be of diagnostic value in focal CD (Gambardella et al., 1996). It is possible that PGA represents the cellular substrate of rhythmic EEG paroxysmal discharges in CD.

Highlights

- Pacemaker GABA synaptic activity (PGA) is a hallmark of pediatric cortical dysplasia.
- PGA occurs in areas with greatest anatomical abnormality.
- PGA is abolished by $GABA_A$ receptor antagonists and sodium channel blockers.
- PGA frequency is ~7.5 Hz and displays high degree of autocorrelation.
- PGA could represent a signal for network synchronization in dysplastic cortex.

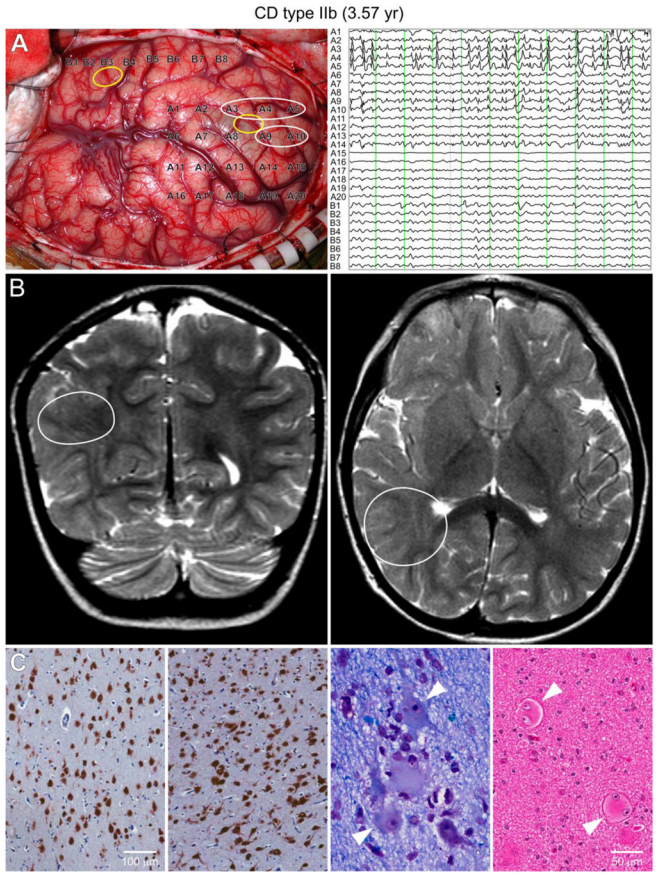

Figure 1.

Type IIb case (3.6 yr) with pharmacoresistant epileptic seizures since the age of 10 m. **A.** During surgery, the ECoG showed continuous epileptic discharges, typical of CD, in the parietal region (white circles) but not in the temporal region. PGA was found in the parietal sample. Yellow circles indicate the areas where the tissue samples for electrophysiology were taken. Each vertical green line on the ECoG trace represents 1 sec. **B.** Coronal (left) and axial (right) MRI T2 scans showing the areas with highest anatomical abnormality (white circles). **C.** The two left panels show NeuN immunostained sections of relatively normally organized neocortex and markedly disorganized neocortex. Disorganized cortex shows crowding and abnormal orientation of many immunoreactive cells (in both pictures the piamater is on top). Calibration applies to both panels. Near right panel: Klüver-Barrera stained section shows dysmorphic neurons with abnormal Nissl substance and cell processes (arrowheads). Far right panel: Hematoxylin and eosin (H&E) stained section showing balloon, binucleated cells (arrowheads). Calibration applies to both panels.

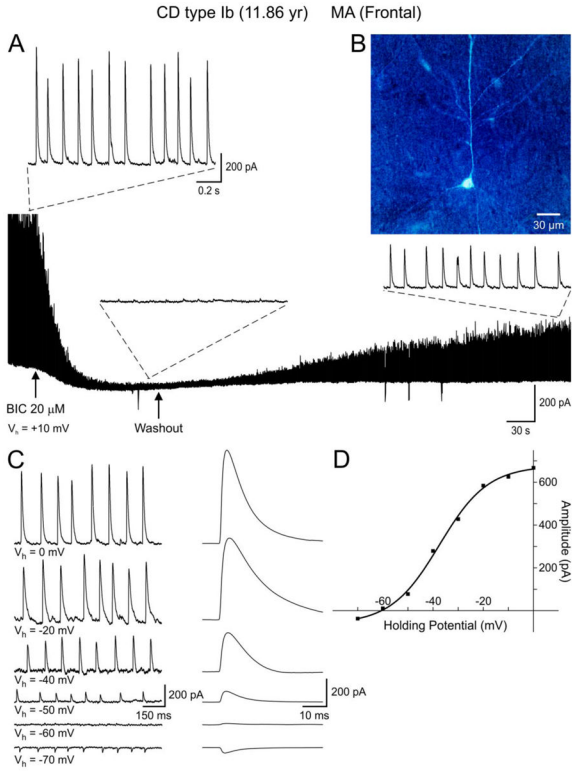

Figure 2.

A. Whole-cell voltage clamp recording demonstrating PGA in a normal-like pyramidal neuron **(B)** from a CD Type Ib case. Pathological analysis revealed cytoarchitectural abnormalities as demonstrated by blurring of most cortical layers. No dysmorphic or "balloon" cells were observed. Bath application of the $GABA_A$ receptor antagonist BIC (20 μM) abolished PGA. After BIC washout PGA slowly recovered. **C.** Holding the membrane at different voltages demonstrated a reversal potential of PGA around −60 mV, which closely corresponds to the predicted reversal potential based on the Cl^- concentration in the internal solution. Traces on the right are the corresponding average of spontaneous GABA synaptic events at different holding potentials. **D.** The current-voltage relationship reveals a reversal potential around −60 mV. Interestingly, the current amplitude values at different holding potentials were better fit with a sigmoid, not a linear, function.

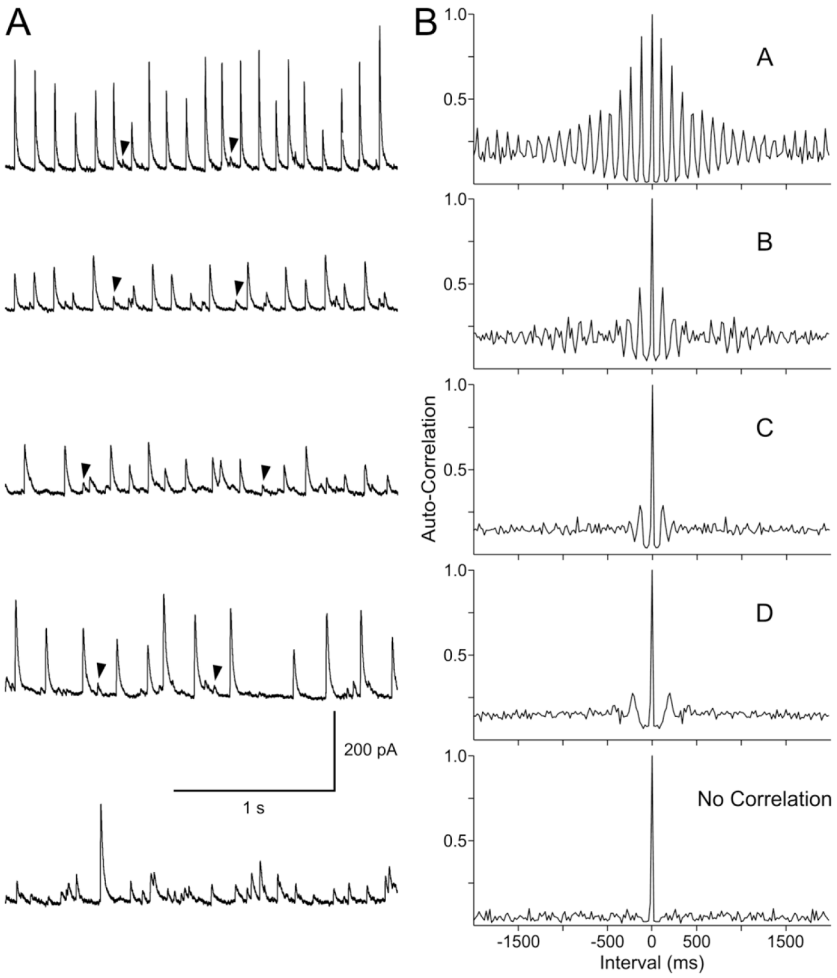

Figure 3.

A. Traces show PGA recorded at a holding potential of +10 mV in pyramidal neurons from different CD Type IIa/b cases. Arrowheads indicate random low-amplitude events. **B.** Autocorrelograms demonstrate the non-random nature of PGA. Depending on the degree of autocorrelation cells were separated into high (A, B) or low (C, D) correlation. The bottom trace and histogram showing the lack of correlation were obtained from a non-PGA pyramidal neuron in a case that presented with PGA.

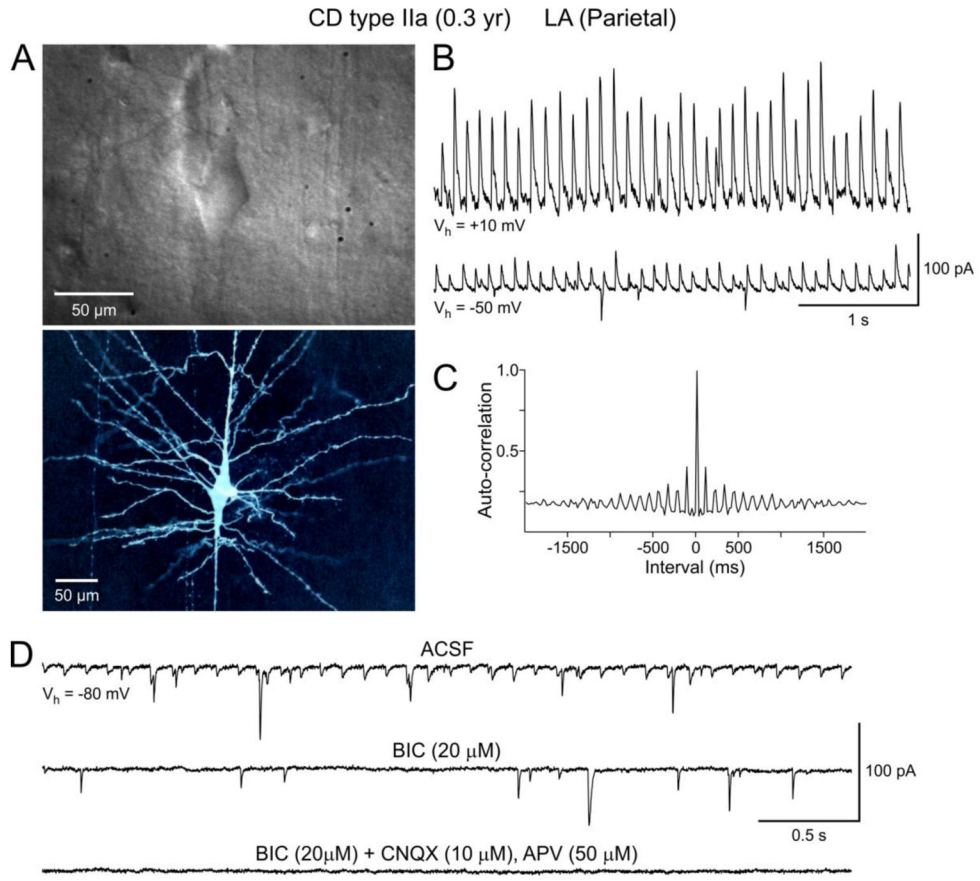

Figure 4.

A. IR-DIC (top panel) and biocytin (lower panel) images of a dysmorphic cytomegalic pyramidal neuron recorded in a CD Type IIa case. **B.** PGA from the cytomegalic neuron shown in **(A).** Downward deflections at V_{hold}=−50 mV are spontaneous glutamatergic synaptic currents. **C.** Autocorrelogram of PGA shown in **(B). D.** At −80 mV this neuron displayed small-amplitude PGA that was blocked after addition of BIC. The remaining events were glutamatergic as they were completely blocked by application of non-NMDA (CNQX) and NMDA (APV) receptor antagonists.

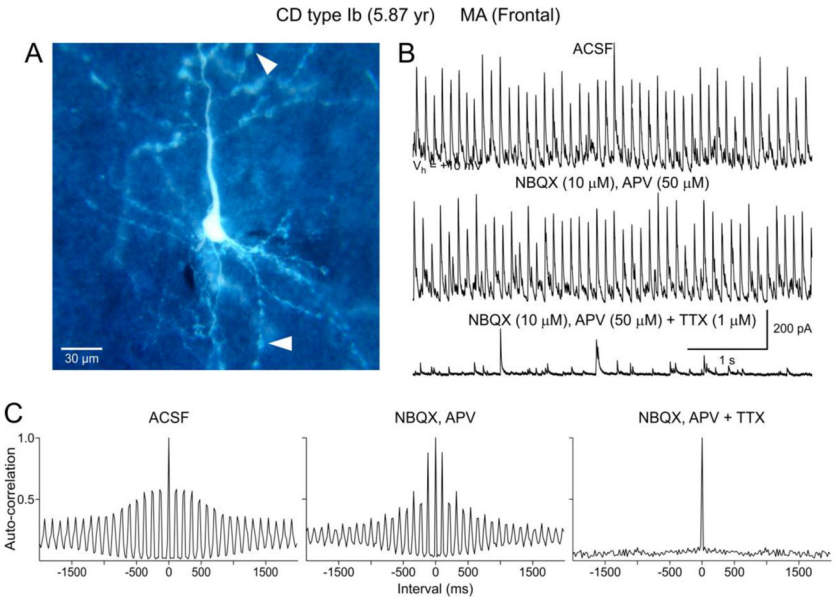

Figure 5.

PGA is dependent on action potentials and is not affected by glutamate receptor blockade. **A.** Normal-sized, biocytin-filled pyramidal neuron from a CD Type Ib case. Arrowheads indicate dendritic blebbing. **B.** PGA recorded at a holding potential of +10 mV in standard solution. Bath application of a selective NMDA receptor antagonist, APV, in conjunction with a non-NMDA receptor antagonist, NBQX, produced no discernible effect on PGA. In contrast, Na^+ channel block with TTX completely abolished PGA, leaving only random mIPSCs. **C.** Autocorrelation histograms associated with traces shown in B. Note the lack of auto-correlation after blockade of Na^+ channels.

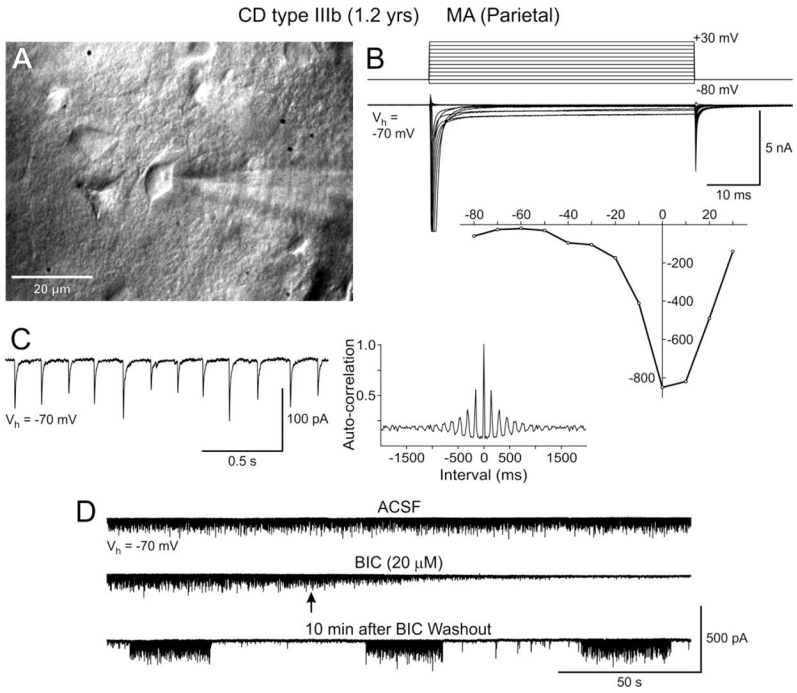

Figure 6.

PGA in an immature neuron from a CD Type IIIb case (CD associated with a ganglioglioma). **A.** IR-DIC image shows a cluster of immature neurons. **B.** Based on the current-voltage relationship, the recorded neuron was likely an immature pyramidal neuron as it displayed inward Na^+ and Ca^{2+} currents to depolarizing voltage commands (Cepeda et al., 2003). **C.** At a holding potential of −70 mV this neuron displayed PGA with a high degree of autocorrelation (A). **D.** PGA was blocked with BIC. Interestingly, upon washout of the $GABA_A$ receptor antagonist PGA occurred in an episodic, rhythmic manner.

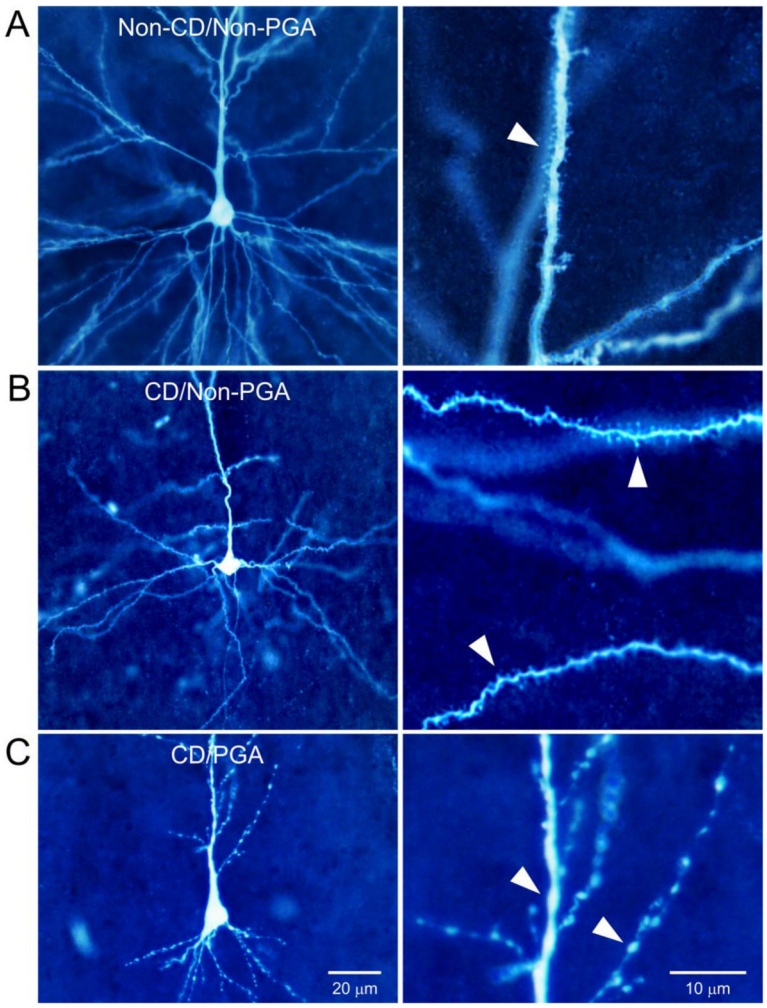

Figure 7.

Morphological changes associated with PGA. **A.** Biocytin-filled normal-like pyramidal neuron from a non-CD case with minimal pathology and Chaslin gliosis. No PGA was observed in this neuron. **B.** Normal-like pyramidal neuron from a CD case that did not display PGA. Morphology was very similar to the normal-like pyramidal neuron from the non-CD case shown in A. No blebbing was observed and spines appeared normal. **C.** Normal-like pyramidal neuron from a CD case that displayed PGA. Notice severe dendritic atrophy and blebbing. Panels on the right are high magnification images from the same neurons shown in the left panels to better appreciate dendritic spines (A and B) and swellings (C).

Table I

PGA in Pediatric Epilepsy Surgical Cases (n=120)

In the present cohort of pediatric epilepsy surgery cases, PGA was observed mostly in CD and TSC cases. PGA occurred in only 2 non-CD cases, one Rasmussen's encephalitis case and one with no remarkable pathology. The difference in the frequency of PGA occurrence between CD and non-CD cases was statistically significant (p=0.01, Chi-square).

	PGA	% Cases
CD (n=80)	**27**	**34%**
CD Type I (n=26)	7	27%
CD Type II (n=50)	17	34%
CD Type III (n=4)	3	75%
TSC (n=15)	**2**	**13%**
Non-CD (n=25)	**2**	**8%**
Rasmussen's Encephalitis (n=8)	1	12.5%
Unremarkable, Chaslin Gliosis (n=6)	1	16.7%
Cystic Infarct (n=2)	0	0%
Cystic-gliotic Encephalopathy (n=3)	0	0%
Heterotopia (n=2)	0	0%
Ulegyria (n=2)	0	0%
Prenatal Stroke (n=1)	0	0%
Sturge-Weber (n=1)	0	0%

Table II

Basic membrane properties of PGA and non-PGA pyramidal neurons. Cell membrane capacitance (Cm), input resistance (Rm), and decay time constant (tau), were similar between both groups.

Basic Membrane Properties of PGA Pyramidal Neurons			
Cell Type	**Cm (pA)**	**Rm (MΩ)**	**Tau (ms)**
Normal-like (n=24)	160.5±14	158.2±23	2.6±0.2
Immature (n=4)	78.0±17	610±214	0.9±0.4
Cytomegalic (n=5)	449.5±54	65.8±28	4.6±0.6

Basic Membrane Properties of Non-PGA Pyramidal Neurons			
	Cm (pA)	**Rm (MΩ)**	**Tau (ms)**
Normal-like (n=128)	159.2±7	213.4±22	2.9±0.2
Immature (n=11)	86.2±7	438.0±93	1.9±0.6
Cytomegalic (n=9)	364.0±35	62.4±8	4.6±0.3